**Supplementary Information**

# Dissecting neural pathways for forgetting in *Drosophila* olfactory aversive memory

Yichun Shuai[1,4], Areekul Hirokawa[1,4], Yulian Ai[1], Min Zhang[1,2], Wanhe Li[3], and Yi Zhong[1]

## Supplementary Figures

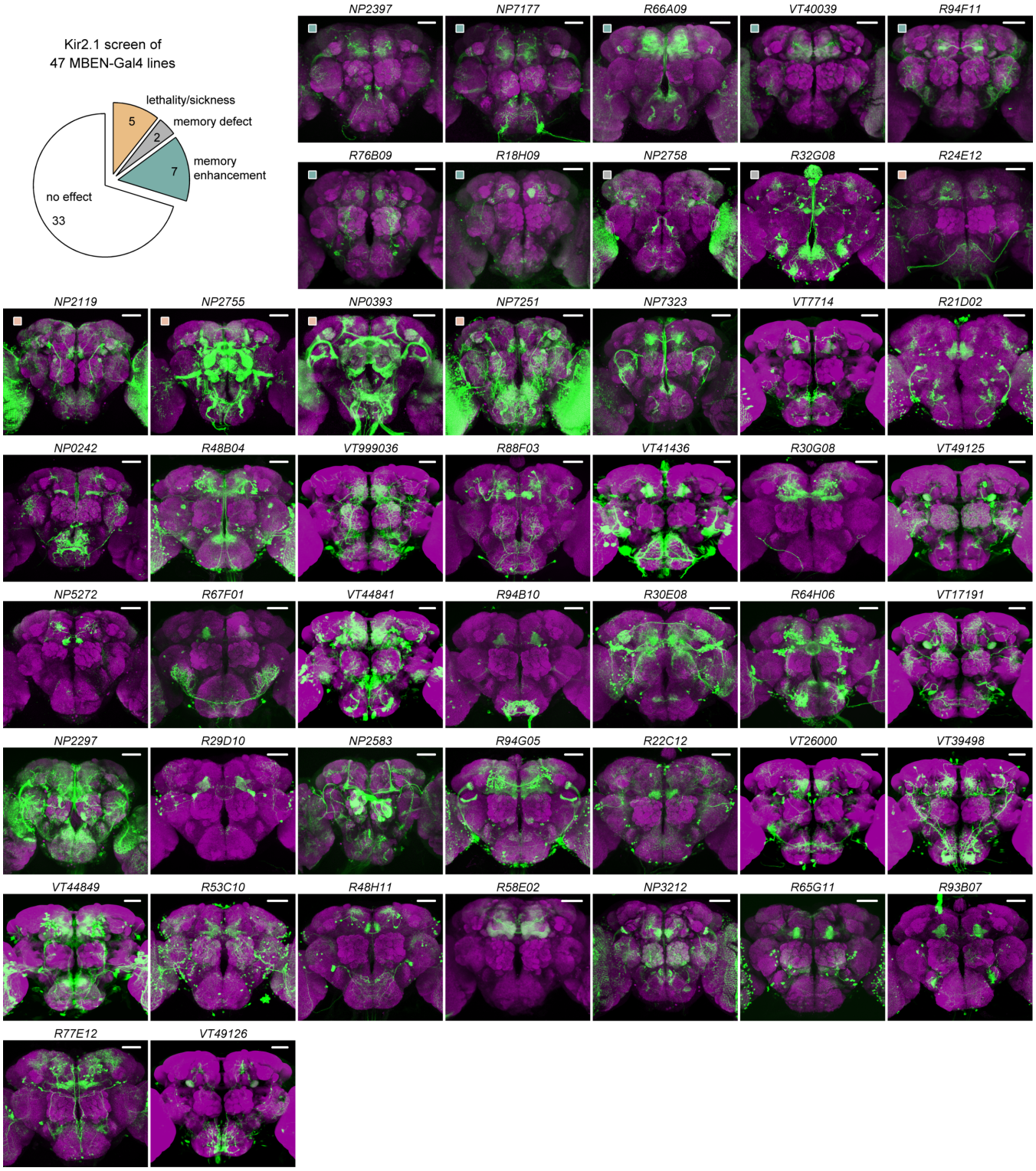


**Figure S1. Screen phenotypes and Gal4 expression patterns in the brain.**

For the screened Gal4 lines, 13 were P{Gal4} enhancer-traps from the NP consortium (1) and were previously characterized to label MBENs (2). The rest were manually selected from Janelia Gal4 (3) and Vienna Tiles (4), two Gal4 collections constructed by linking Gal4 with a fragment of genomic DNA (5). The Gal4 lines showing screen phenotypes are indicated by colored squares. Neuropils were labeled with the nc82 antibody (magenta). Scale bars are 50 μm.

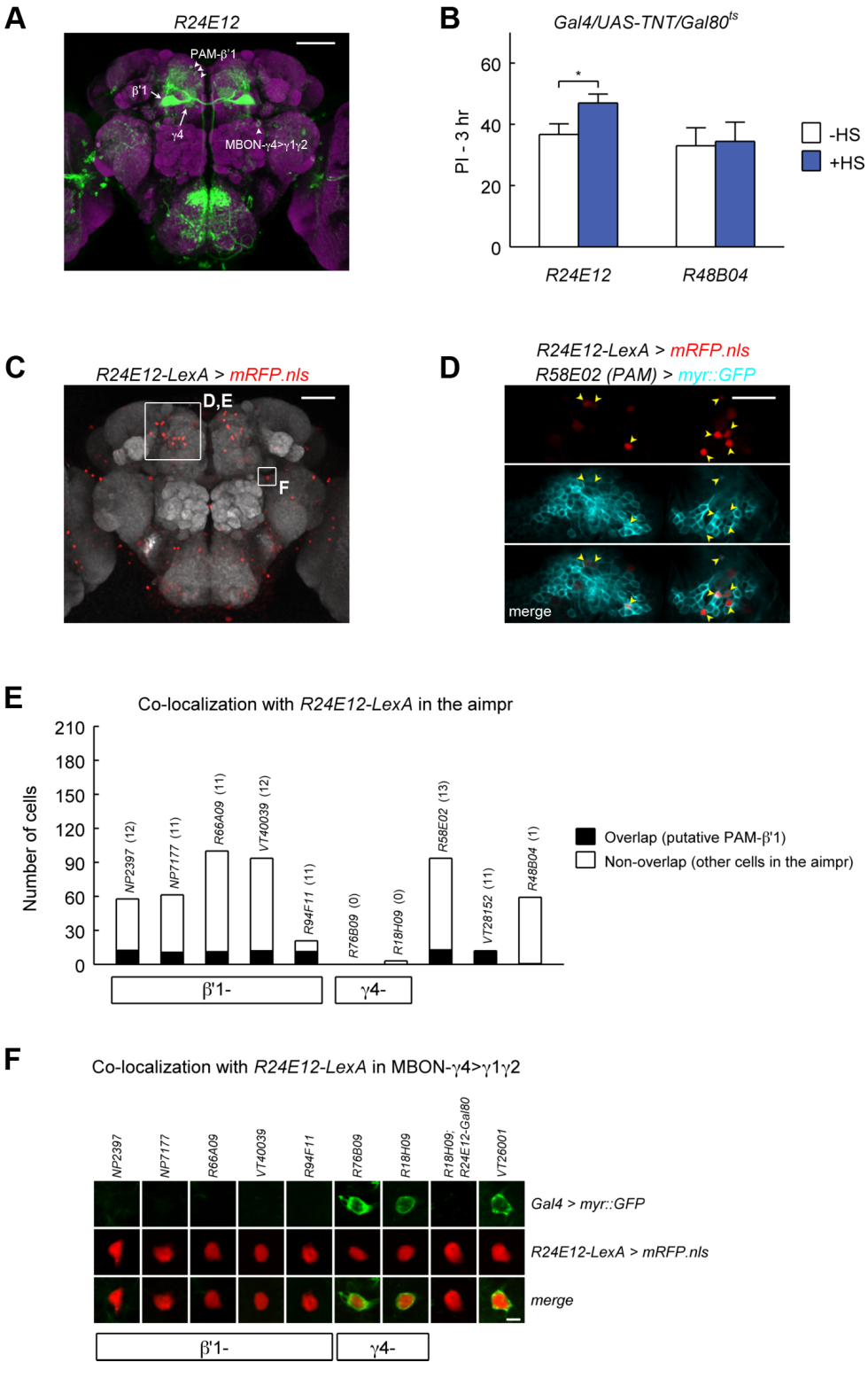


**Figure S2. *R24E12* is expressed in two MBEN types shared with Gal4 lines identified from the screen.**

(**A**) *R24E12*-driven *UAS-IVS-myr::GFP* expression in the brain. The two MBEN types, PAM-β'1 and MBON-γ4>γ1γ2, are indicated.
(**B**) Blocking *R24E12*-neurons but not *R48B04*-neurons increased 3 hr memory retention (*R24E12*, p = 0.03, n = 13; *R48B04*, p = 0.87, n = 8; t-test). TNT, the light chain of tetanus toxin, was used for neuronal blockade, because *R24E12*-driven Kir2.1 expression caused partial lethality in adult flies. See **Fig. 3I** and **SI Appendix, Fig. S2E** for expression of the *R48B04* driver. Data are means ± s.e.m. *, p < 0.05.
(**C**) *R24E12-LexA*-driven expression of a nucleus-localized RFP reporter (mRFP.nls). This LexA (6) driver was used as a Gal4-independent genetic landmark to locate the PAM-β'1 somas in the anterior inferior medial protocerebrum (aimpr) in (**D**,**E**) and to locate the MBON-γ4>γ1γ2 somas in (**F**).
(**D**) Cells visualized by *R24E12-LexA* in the aimpr were mostly PAM-β'1 neurons. In this brain area, *R24E12-LexA* labeled 18 ± 1 cells on each hemisphere; 13 ± 1 of these cells were double-labeled by the PAM-specific *R58E02* Gal4 (means ± s.e.m., n = 4 hemispheres). Representative images are single confocal sections of two-color imaging of *R24E12-LexA* and *R58E02* in the aimpr. Arrowheads indicate double-labeled cells.

(**E**) Examination of PAM-β'1 expression across Gal4 drivers. Numbers indicate Gal4-expressing cells in the aimpr that were co-localized with *R24E12-LexA* in two-color imaging. Data are means from 2-8 hemispheres.
(**F**) Examination of MBON-γ4>γ1γ2 expression across Gal4 drivers. Representative images are single confocal sections of MBON-γ4>γ1γ2 soma.
Neuropils were labeled with the nc82 antibody (magenta in **A**, gray in **C**). Scale bars are 50 μm (**A**,**C**), 20 μm (**D**) and 5 μm (**F**).

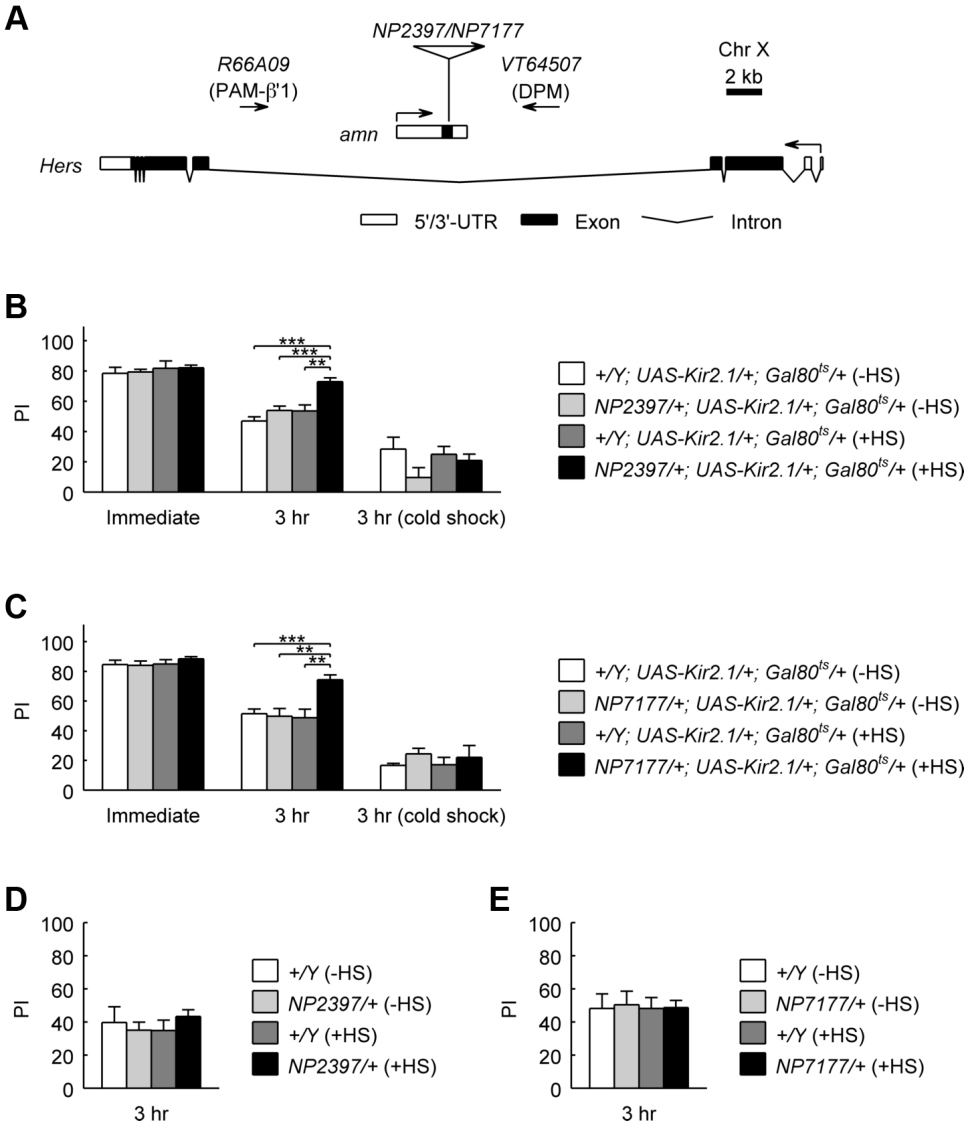


**Figure S3. Additional controls for the two PAM-β'1 lines *NP2397* and *NP7177*.**

(**A**) *NP2397* and *NP7177* carry P{Gal4} enhancer traps inserted in the exon of *amn* with insertion sites that are one base pair from each other (1). *R66A09,* another PAM-β'1 line in the screen (**Fig. 1B**), carries a 1.6-kb genomic enhancer fragment at 7.2 kb upstream of *amn* (5). None of these three lines have expression in the DPM neurons. However, the DPM neurons are labeled in one Gal4 line (*VT64507*) carrying a genomic enhancer fragment downstream of *amn* (data released by Vienna Tiles). Different regulatory sequences flanking *amn* may separately drive the expression in the DPM and PAM-β'1 neurons.

(**B**) The inactivation of *NP2397*-neurons with Kir2.1 suppressed forgetting of early labile memory. Kir2.1 was expressed in *NP2397*-neurons in HS-treated female flies that carried the combination of Gal4 drivers with *UAS-Kir2.1; Gal80$^{ts}$*. This experimental group, *NP2397/+; UAS-Kir2.1/+; Gal80$^{ts}$*/+ (+HS), was compared the -HS control group as well as the male sibling groups lacking a Gal4 driver [*+/Y; UAS-Kir2.1/+; Gal80$^{ts}$*/+ (+HS)/(–HS)]. The learning

performance was not different among the tested groups ($p = 0.83$, $n = 8$, one-way ANOVA), but 3 hr memory retention was significantly higher in the experimental group ($p < 0.01$ for vs. all three controls, $n = 28$, one-way ANOVA/Bonferroni). The differences in 3 hr memory retention were suppressed by a 2-min cold shock applied at 2 hr after training ($p = 0.28$, $n = 10$, one-way ANOVA). For "3 hr without cold shock", data from screen ($n = 6$, **SI Appendix, Table S1**) and replication ($n = 22$, **Fig. 1D**) were combined.

(**C**) The inactivation of *NP7177*-neurons with Kir2.1 showed consistent phenotypes as the inactivation of *NP2397*-neurons. The experimental group, *NP7177/+; UAS-Kir2.1/+; Gal80$^{ts}$/+* (+HS), had normal learning performance ($p = 0.65$, $n = 8$, one-way ANOVA), but significantly better 3 hr memory retention ($p < 0.01$ for vs. all three controls, $n = 12$, one-way ANOVA/Bonferroni). The 3 hr memory differences were blocked by cold shock ($p = 0.39$, $n = 10$, one-way ANOVA). For "3 hr without cold shock", data from screen ($n = 6$, **SI Appendix, Table S1**) and replication ($n = 6$, **Fig. 1E**) were combined.

(**D**-**E**) Female heterozygotes of *NP2397* and *NP7177* showed normal 3 hr memory performance irrespective of HS-treatment. No differences were found among the tested groups (For *NP2397*, $p = 0.76$, $n = 6$; for *NP7177*, $p > 0.95$, $n = 6$; one-way ANOVA).

Data in **B**-**E** are means ± s.e.m. **, $p < 0.01$. **, $p < 0.001$.

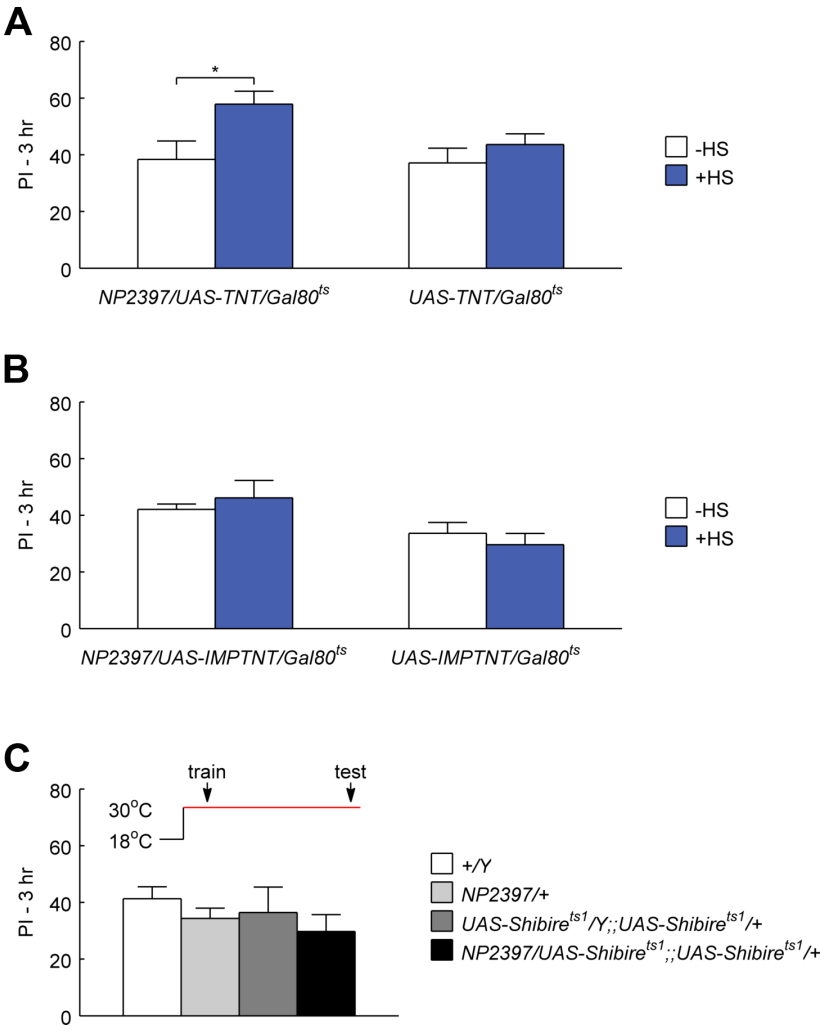


**Figure S4. Inactivation of *NP2397*-neurons using different effectors.**

(**A**) Blocking synaptic output of *NP2397*-neurons by induced expression of tetanus toxin light chain (TNT) in adult flies led to increased 3 hr memory retention. For *NP2397/+; UAS-TNT/+; Gal80$^{ts}$/+*, p = 0.03, n = 8, t-test. For the male siblings without the Gal4 driver (*+/Y; UAS-TNT/+; Gal80$^{ts}$/+*), p = 0.33, n = 8, t-test.

(**B**) Expression of a mutationally inactivated tetanus toxin light chain (IMPTNT) in *NP2397*-neurons did not have an effect on 3 hr memory. For *NP2397/+; UAS-IMPTNT/+; Gal80$^{ts}$/+*, p = 0.55, n = 8, t-test. For the male siblings *+/Y; UAS-IMPTNT/+; Gal80$^{ts}$/+*, p = 0.48, n = 8, t-test.

(**C**) Expression of Shibire$^{ts1}$ in *NP2397*-neurons did not cause a 3 hr memory phenotype (p = 0.61, n = 6, one-way ANOVA). Flies were cultured and collected at 18$^{o}$C and assayed for memory performance at 30$^{o}$C, a restrictive temperature at which Shibire$^{ts1}$ interferes with synaptic vesicle recycling and neuronal output. As indicated in the schematic, flies were transferred to 30$^{o}$C at 30 min before training and stayed throughout.

Data are means ± s.e.m. *, p < 0.05.

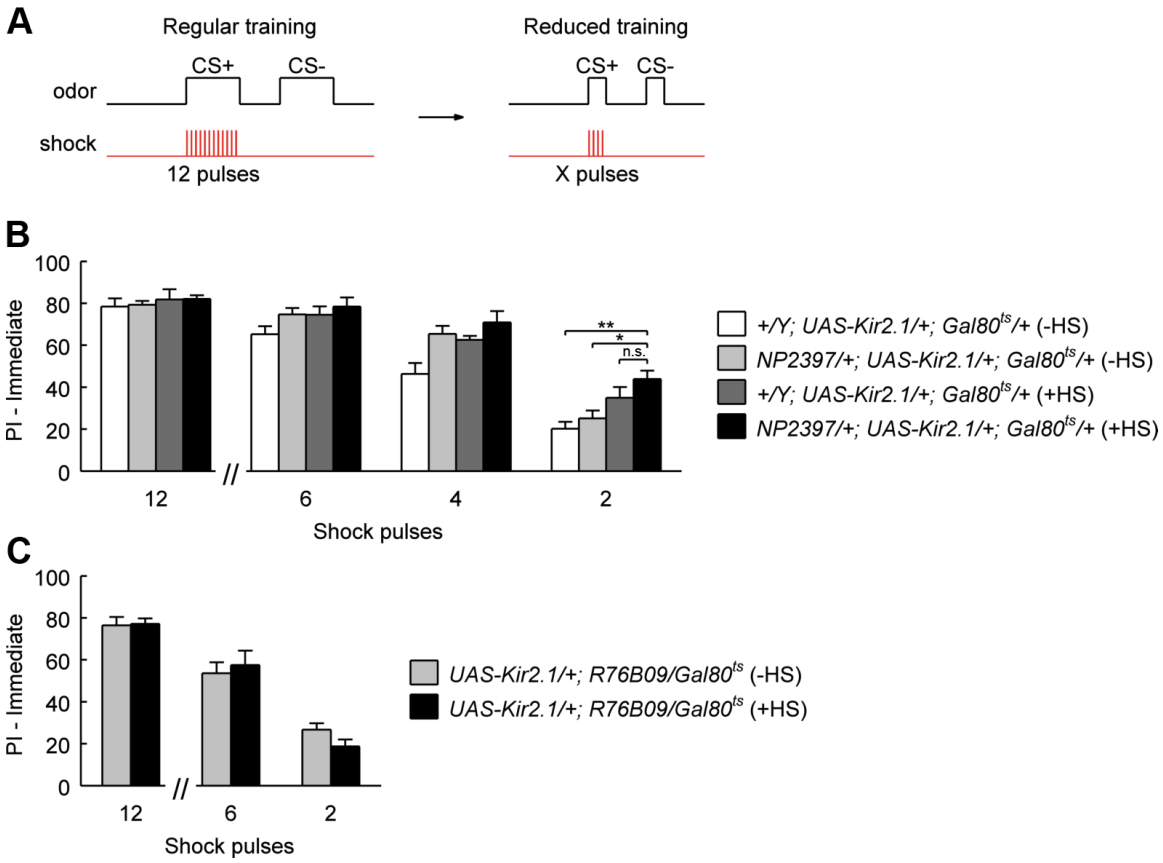


**Figure S5. Learning performance under conditions of reduced training.**

(**A**) Training intensity was reduced by decreasing the number of delivered electric shock pulses, from the regular 12 to 6, 4 and 2; odor durations were correspondingly shortened. Learning performance was assayed immediately after training.

(**B**) Flies expressing Kir2.1 under the PAM-β'1 driver *NP2397* had learning performance comparable to controls. Under the conditions of "6 pulses" and "4 pulses", the experimental group, the HS-treated *NP2397/+; UAS-Kir2.1/+; Gal80$^{ts}$/+* flies, had learning performance not significantly different from any of the three controls ["6 pulses", $p > 0.11$, $n = 8$, one-way ANOVA; "4 pulses", $p = 0.05$ for vs. "+/Y; *UAS-Kir2.1/+; Gal80$^{ts}$/+* (-HS)", $p > 0.95$ for vs. the other two controls, $n = 6$, one-way ANOVA/Bonferroni]. Under the condition of "2 pulses", the experimental group showed learning performance similar to the HS-treated male siblings lacking a Gal4 driver [for vs. "+/Y; UAS-Kir2.1/+; Gal80ts/+ (+HS)", $p > 0.95$, $n = 12$, one-way ANOVA/Bonferroni], although the performance is higher than the two "-HS" controls [for vs. "*NP2397/+; UAS-Kir2.1/+; Gal80ts/+* (-HS)", $p = 0.02$; for vs. *"+/Y; UAS-Kir2.1/+; Gal80ts/+* (-HS)", $p = 0.001$; $n = 12$, one-way ANOVA/Bonferroni].

(**C**) Expression of Kir2.1 with the MBON-γ4>γ1γ2 driver *R76B09* did not affect learning performance under conditions of reduced training ("6 pulses", $p = 0.66$, $n = 6$; "2 pulses", $p = 0.11$, $n = 6$; t-test).

Data are means ± s.e.m. *, $p < 0.05$. **, $p < 0.01$. n.s., not significant.

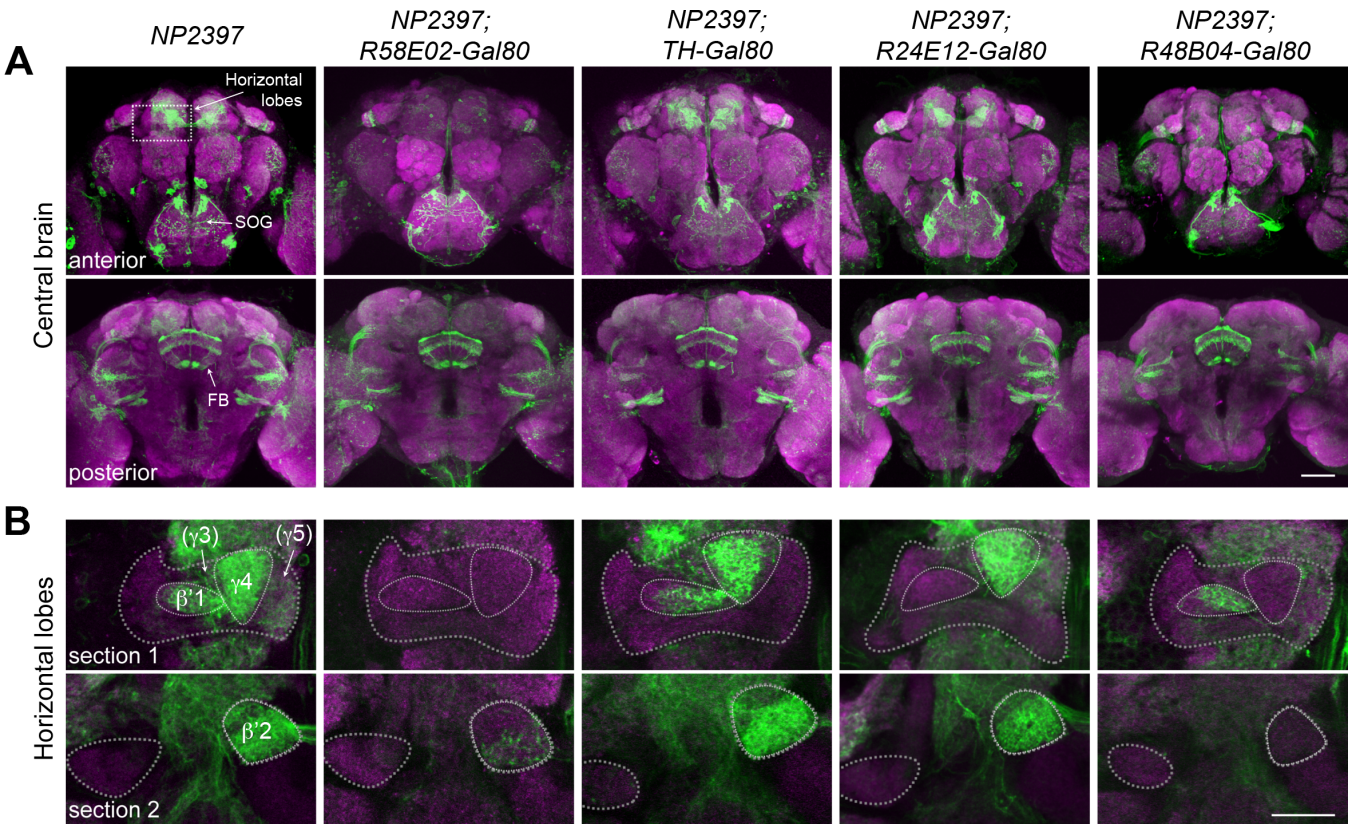


**Figure S6. Refinement of *NP2397* expression pattern using a Gal80 intersectional strategy.**

(**A**) Projection of the central brain. Other than PAM-DANs innervating the MB horizontal lobes, the expression of *NP2397* elsewhere in the brain, e.g. the fan-shaped body (FB) and the subesophageal ganglion (SOG), was not significantly altered by the panel of Gal80 lines used. (**B**) Single confocal sections showing magnified views of the horizontal lobes. The two section planes were chosen to represent the lobe compartments innervated by distinct PAM subsets in *NP2397*. PAM-selective *R58E02-Gal80* removed the expression of *NP2397* in all lobe compartments except for some sparse expression in β'2. For the two Gal80 lines used to target specific PAM subsets in *NP2397*, the behavior-rescuing *R24E12-Gal80* specifically removed the expression in PAM-β'1, while the non-rescuing *R48B04-Gal80* removed the expression in PAM-γ4, β'2, but left the expression in PAM-β'1 intact. *NP2397* also showed weak but detectable expression in γ3 and γ5, which perhaps also came from PAM-DANs. The expression in γ3 and γ5 was removed by *R48B04-Gal80* and *TH-Gal80* respectively, but both Gal80 lines failed in the rescue experiment (**Fig. 3G**). It is worth mentioning that the GFP expression of *NP2397* does not occupy the whole β'1 compartment (compare GFP to the β'1 boundary defined by nc82 counterstaining). PAM-β'1 neurons can be further divided into two subtypes, PAM-β'$1_{ap}$ and PAM-β'$1_{m}$, depending on their innervated β' lobe stratum (7). *NP2397*, as well as *NP7177*, preferentially labeled the PAM-β'$1_{ap}$ subtype (2), while other

PAM-β’1 Gal4 drivers identified from the screen seemed non-selective. Limited by available genetic tools, we did not further distinguish the two PAM-β’1 subtypes in the present study. Neuropils were labeled with the nc82 antibody (magenta). Scale bars are 50 μm (**A**) and 20 μm (**B**).

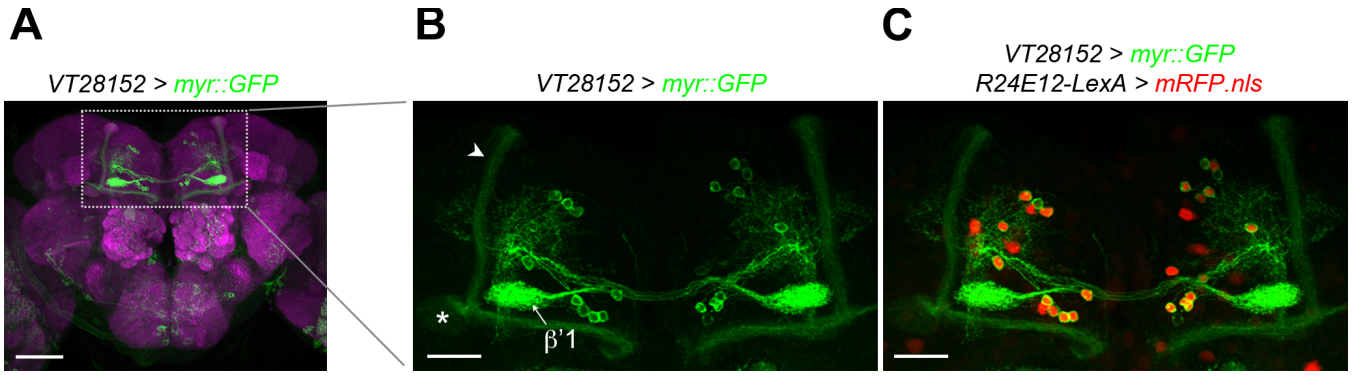


**Figure S7. VT28152 labels PAM-DANs specific to the PAM-β'1 subset.**
(**A**) Projection of *VT28152* expression pattern in the brain. Neuropils were labeled with the nc82 antibody (magenta).
(**B**) Magnified view of the brain region including the MB lobes. PAM-DANs in *VT28152* innervated only β'1. Besides PAM-β'1, *VT28152* also sparsely labeled $KC_{\alpha/\beta}$ (arrowhead) and had faint, stochastic expression in MBON-γ1pedc>α/β (asterisk in the γ1 of the right hemisphere). (**C**) Co-localization of *VT28152* (green) with the PAM-β'1 marker, *R24E12-LexA* (red), in two-color imaging. See **SI Appendix, Fig. S2E** for quantification.
Scale bars are 50 μm (**A**) and 20 μm (**B,C**).

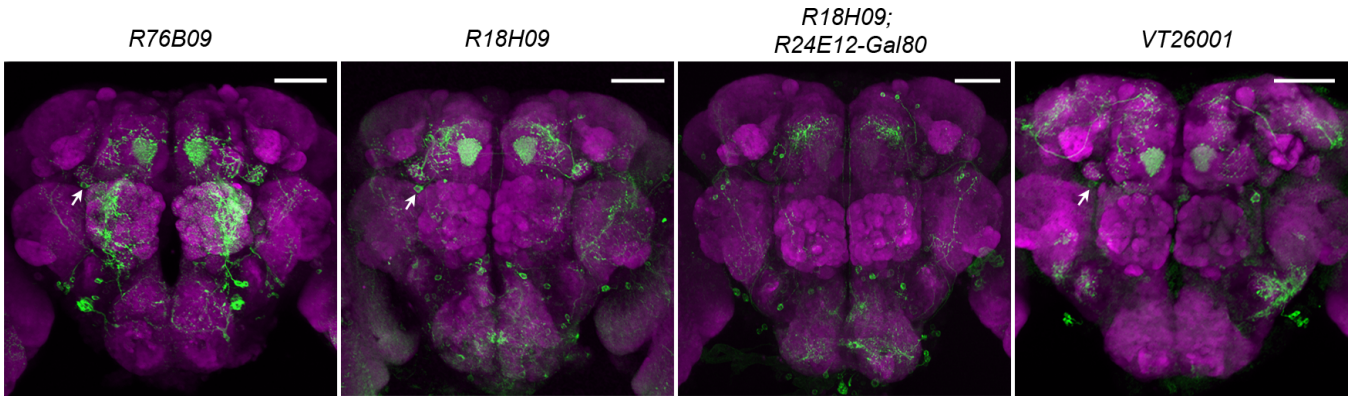


**Figure S8. Brain expression patterns for Gal4 lines related to MBON-γ4>γ1γ2.**
Arrow indicates MBON-γ4>γ1γ2 in the two lines identified from the screen (*R76B09* and *R18H09*) and in a Gal4 line for validation (*VT26001*). The combination of *R18H09* with *R24E12-Gal80* removed the expression in MBON-γ4>γ1γ2, but did not significantly alter expression elsewhere in the brain. Neuropils were labeled with the nc82 antibody (magenta). Scale bars are 50 μm.

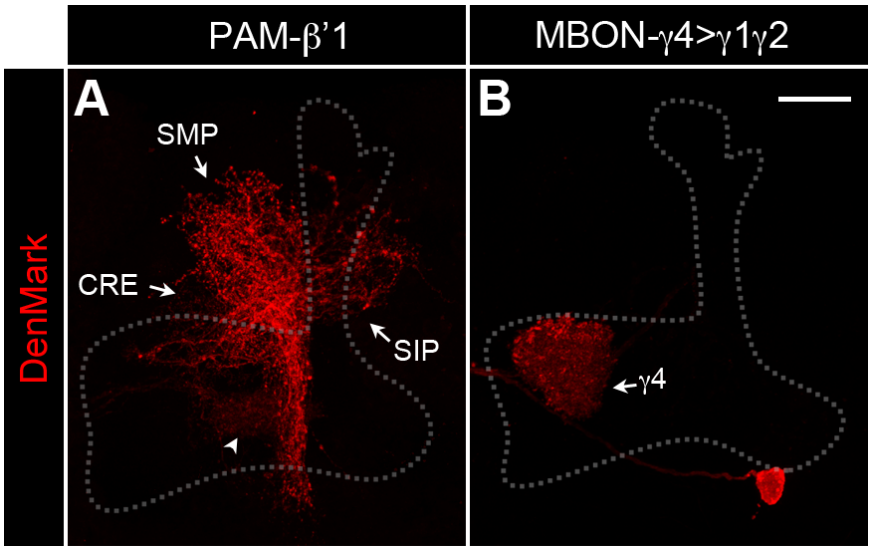


**Figure S9. Distribution of the dendritic marker DenMark in PAM-β'1 and MBON-γ4>γ1γ2.** Images are projection of the brain region including the MB lobes (gray dashed line). For PAM-β'1, DenMark labeling was enriched in neurites outside the MB in the SMP, SIP and CRE areas, although a weak level of DenMark labeling was also detected in β'1 (arrowhead). For MBON-γ4>γ1γ2, DenMark labeling was found in γ4, but not in other γ lobe compartments or in projection areas outside the MB. PAM-β'1 somas obscured the DenMark distribution pattern and were artificially removed. Scale bar is 20 μm. Genotypes are *UAS-DenMark > R94F11-Gal4DBD; R24E12-p65AD* (**A**) and *UAS-DenMark > R76B09-Gal4DBD; R24E12-p65AD* (**B**).

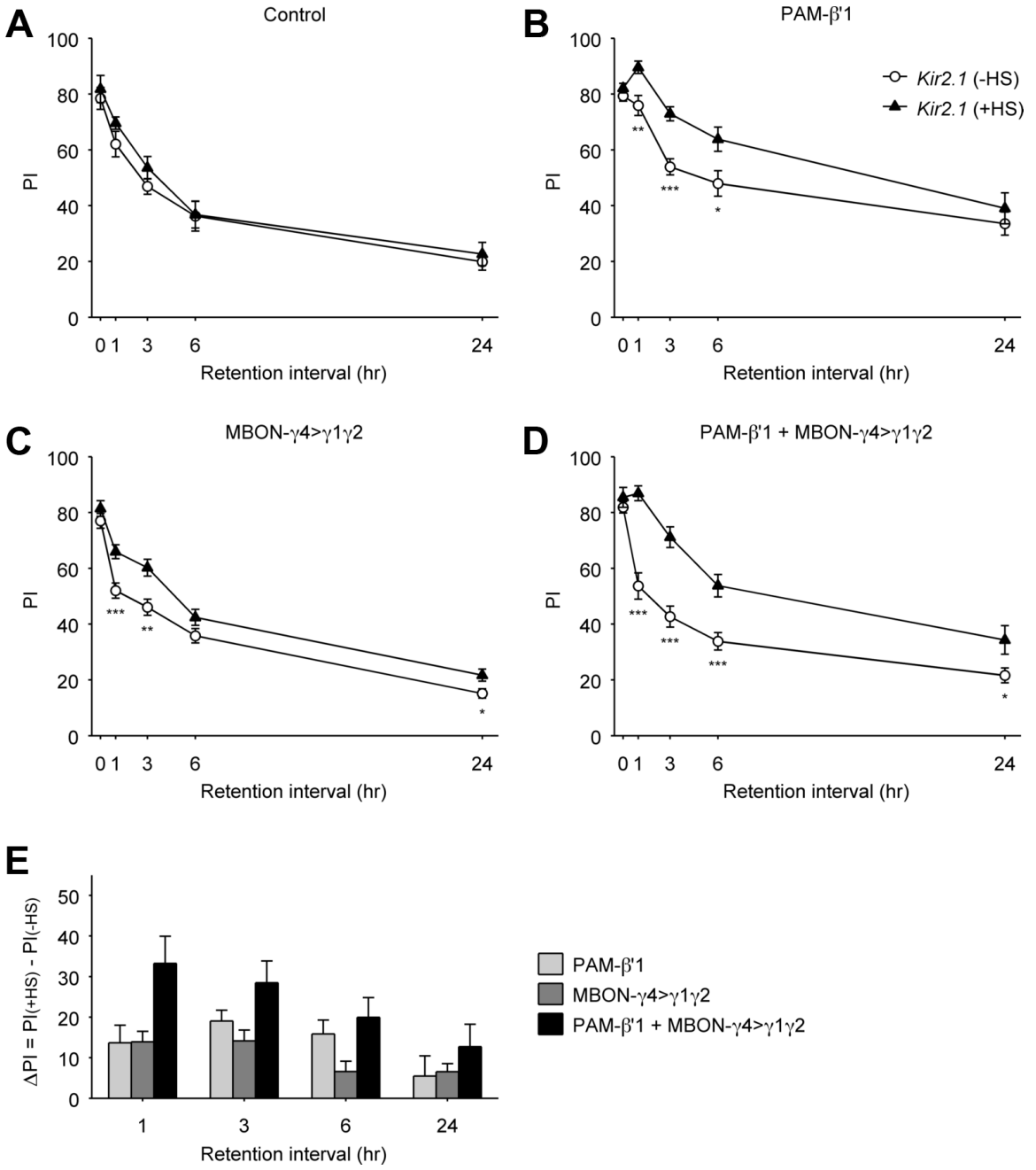


**Figure S10. Combinatorial inactivation of PAM-β'1 and MBON-γ4>γ1γ2 has a stronger effect in inhibiting memory decay.**

(**A**-**D**) Memory decay curves of Kir2.1-inactivation of PAM-β'1, MBON-γ4>γ1γ2 and their combination. "Control" had no Gal4 driver. Experimental groups were from *NP2397* (PAM-β'$_1$), *R76B09* (MBON-γ4>γ1γ2) and *NP2397; R76B09* (PAM-β'$_1$ + MBON-γ4>γ1γ2). The +HS and –HS groups were subjected to comparison at different time points after single-session training. All statistically significant differences (t-test) are marked. *, $p < 0.05$. **, $p < 0.01$. ***, $p < 0.001$. $n \geq 6$.

(**E**) ΔPI between the +HS and –HS groups. Memory curves of –HS control groups of different genotypes in (**A**-**D**) showed considerable variation, which might arise from different genetic background or data acquisition at discrete time. To equilibrate these differences, ΔPI was calculated and taken as an indicator of the effects of neuronal inactivation on memory retention. Depicted are ΔPI from three neuron groups (PAM-β'1, MBON-γ4>γ1γ2, and the combination) and four retention intervals (1, 3, 6 and 24 hr). These data were subjected to a two-way ANOVA with NEURON ($F_{(2, 244)}$ = 11.21, $p < 0.001$) and INTERVAL ($F_{(3, 244)}$ = 6.24, $p < 0.001$) as main effects and NEURON × INTERVAL ($F_{(6, 244)}$ = 0.91, $p = 0.49$) as the interaction term. The combinatorial neuron group was statistically significantly different from the two individual neuron groups as analyzed by multiple comparisons of population marginal means (Multcompare) in MATLAB with significance level set at 0.01.

Data are means ± s.e.m.

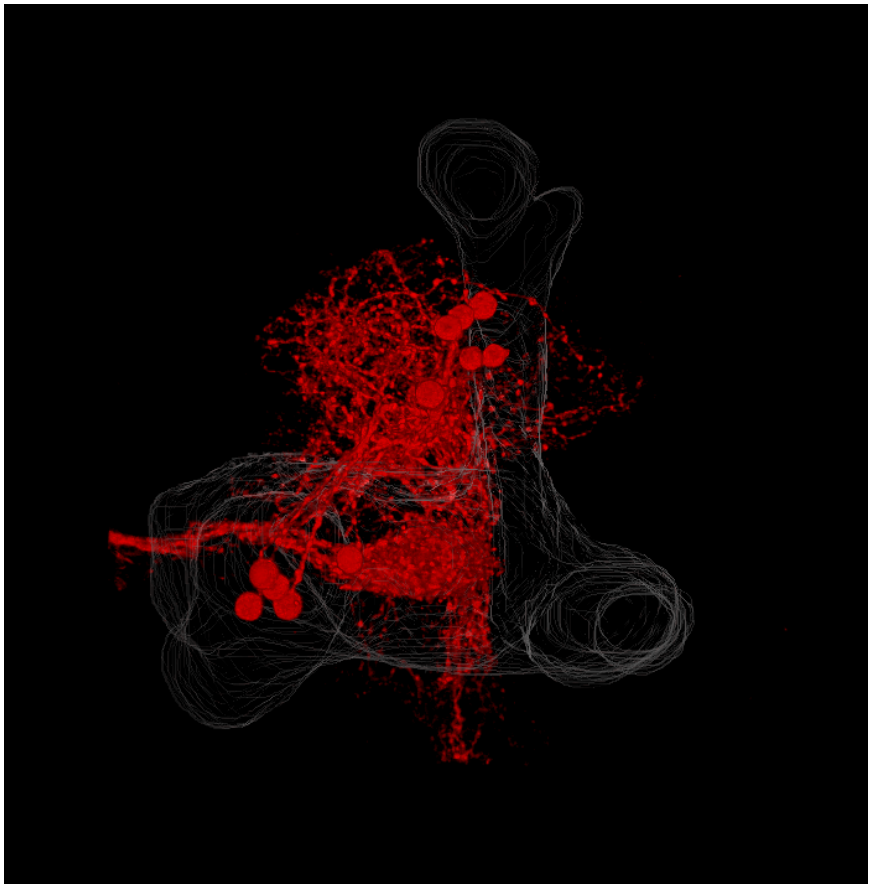

**Video S1. 3D reconstruction of PAM-β’1.**

*R94F11-Gal4DBD; R24E12-p65AD* > *UAS-IVS-mCD8::RFP*. See **Fig. 5** legend.

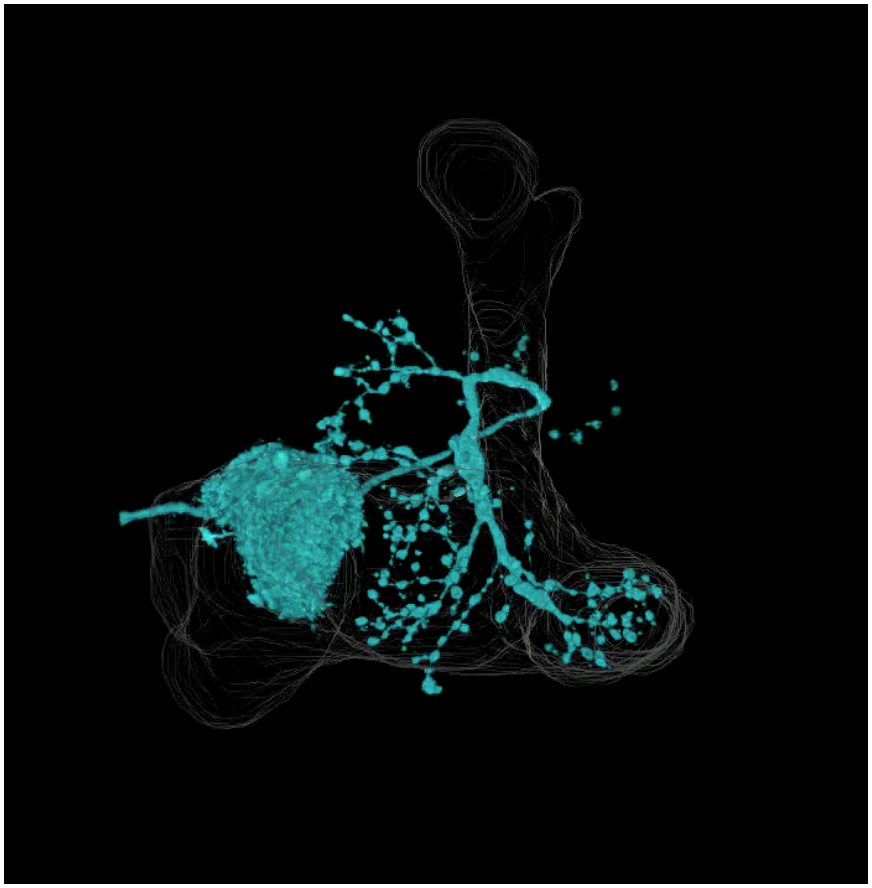

**Video S2. 3D reconstruction of MBON-γ4>γ1γ2.**

*R76B09-LexA > LexAop2-mCD8::GFP*. See **Fig. 5** legend.

## Table S1. Three-hour memory screen of MBEN Gal4 driver lines.

| Gal4 | PI (mean ± s.e.m.) | | ΔPI | n | p value | Innervated lobe compartments | | | | Tanaka et al. 2008 | Chr | Source |
|---|---|---|---|---|---|---|---|---|---|---|---|---|
| | - HS | + HS | | | | γ | β | β' | α/ α' | | | |
| *no Gal4* | 45 ± 3 | 48 ± 4 | 2 | 12 | 0.63 | | | | | | | |
| *NP2758* | 35 ± 5 | 7 ± 4 | -28 | 6 | < 0.01 | γ1 | | | | MB-MP1 | X | DGRC-Kyoto |
| *R32G08* | 51 ± 5 | 25 ± 4 | -26 | 6 | < 0.01 | | β12 | (β'2) | | | 3 | BDSC |
| *NP7323* | 48 ± 6 | 38 ± 6 | -10 | 6 | 0.27 | γ34 | | β'1 | | MB-M2 | 2 | DGRC-Kyoto |
| *VT7714* | 47 ± 5 | 39 ± 5 | -7 | 6 | 0.31 | γ3 | | β'1 | | | 3 | VDRC |
| *R21D02* | 40 ± 5 | 33 ± 5 | -7 | 6 | 0.36 | γ5 | β2 | β'2 | | | 3 | BDSC |
| *NP0242* | 52 ± 4 | 46 ± 1 | -6 | 6 | 0.19 | | β1(2) | | (α123) | MB-MV2 | 3 | DGRC-Kyoto |
| *R48B04* | 35 ± 3 | 29 ± 3 | -6 | 9 | 0.22 | γ(3)45 | | β'2 | | | 3 | BDSC |
| *VT999036* | 45 ± 6 | 42 ± 5 | -3 | 4 | 0.74 | γ(12)45 | | | | | 3 | Barry Dickson |
| *R88F03* | 43 ± 9 | 42 ± 5 | -2 | 6 | 0.85 | | | β'2 | | | 3 | BDSC |
| *VT41436* | 42 ± 3 | 42 ± 2 | 0 | 6 | 0.96 | γ3 | | β'1 | | | 3 | VDRC |
| *R30G08* | 30 ± 8 | 30 ± 5 | 0 | 6 | 0.98 | γ34(5) | β1(2) | β'(1)2 | α1 | | 3 | BDSC |
| *VT49125* | 63 ± 4 | 63 ± 3 | 0 | 4 | 0.96 | γ1 | | | | | 3 | VDRC |
| *NP5272* | 38 ± 5 | 39 ± 5 | 1 | 6 | 0.92 | | β2 | (β'2) | | MB-M3 | 2 | DGRC-Kyoto |
| *R67F01* | 39 ± 5 | 39 ± 5 | 1 | 6 | 0.91 | γ3 | | β'1 | | | 3 | BDSC |
| *VT44841* | 28 ± 10 | 30 ± 6 | 2 | 5 | 0.84 | γ(123)45 | | (β'2) | α1 | | 3 | VDRC |
| *R94B10* | 39 ± 5 | 41 ± 4 | 2 | 6 | 0.79 | γ3 | | β'1 | | | 3 | BDSC |
| *R30E08* | 39 ± 8 | 40 ± 4 | 2 | 4 | 0.88 | γ(12)4 | β1 | | (α123) | | 3 | BDSC |
| *R64H06* | 41 ± 5 | 43 ± 3 | 2 | 11 | 0.78 | γ(1)345 | β12 | β'12 | | | 3 | BDSC |
| *VT17191* | 60 ± 5 | 62 ± 3 | 2 | 4 | 0.75 | γ1 | | | | | 3 | VDRC |
| *NP2297* | 38 ± 4 | 41 ± 5 | 3 | 6 | 0.61 | γ5 | β12 | β'2 | | MB-M1/-M7/-CP1 | 2 | DGRC-Kyoto |
| *R29D10* | 36 ± 4 | 40 ± 4 | 3 | 6 | 0.58 | γ3 | | β'1 | | | 3 | BDSC |
| *NP2583* | 47 ± 2 | 52 ± 2 | 5 | 6 | 0.13 | | β1 | | α1 | MB-MVP1 | 2 | DGRC-Kyoto |
| *R94G05* | 38 ± 2 | 43 ± 2 | 5 | 8 | 0.13 | γ(12)345 | | β'12 | | | 3 | BDSC |
| *R22C12* | 34 ± 6 | 39 ± 6 | 5 | 6 | 0.57 | γ2 | β2 | (β'2) | α'1 | | 3 | BDSC |
| *VT26000* | 37 ± 7 | 43 ± 3 | 6 | 5 | 0.42 | γ(12)4 | β1 | | α2/α'2? | | 3 | VDRC |

| | | | | | | | | | | | | |
|---|---|---|---|---|---|---|---|---|---|---|---|---|
| *VT39498* | 36 ± 5 | 43 ± 5 | 7 | 6 | 0.29 | γ4 | | | | | 3 | VDRC |
| *VT44849* | 23 ± 5 | 30 ± 6 | 7 | 9 | 0.38 | γ1245 | | β'2 | α1 | | 3 | VDRC |
| *R53C10* | 33 ± 5 | 40 ± 3 | 7 | 6 | 0.25 | γ(12)4 | β1 | β'2 | (α123) | | 3 | BDSC |
| *R48H11* | 39 ± 3 | 45 ± 3 | 7 | 6 | 0.15 | γ5 | | | | | 3 | BDSC |
| *R58E02* | 44 ± 6 | 52 ± 4 | 8 | 6 | 0.26 | γ(12)345 | β12 | β'12 | α1 | | 3 | Hiromu Tanimoto |
| *NP3212* | 44 ± 4 | 53 ± 6 | 9 | 6 | 0.25 | γ35 | | β'2 | | MB-M4/M5/-M6 | 3 | DGRC-Kyoto |
| *R65G11* | 39 ± 6 | 48 ± 2 | 9 | 8 | 0.22 | γ3 | β1 | β'1 | | | 3 | BDSC |
| *R93B07* | 30 ± 4 | 40 ± 3 | 9 | 8 | 0.10 | γ3 | | β'1 | | | 3 | BDSC |
| *R77E12* | 29 ± 5 | 39 ± 5 | 10 | 6 | 0.21 | γ5 | β1(2) | β'2 | | | 3 | BDSC |
| *VT49126* | 47 ± 4 | 58 ± 4 | 11 | 6 | 0.09 | γ1 | | | | | 3 | VDRC |
| *R18H09* | 33 ± 1 | 49 ± 3 | 16 | 6 | < 0.001 | γ(12)4 | | | | | 3 | BDSC |
| *R94F11* | 35 ± 4 | 52 ± 3 | 16 | 8 | < 0.01 | γ13 | | β'1 | (α3) | | 3 | BDSC |
| *R66A09* | 43 ± 4 | 62 ± 3 | 19 | 8 | < 0.01 | γ1345 | β12 | β'12 | | | 3 | BDSC |
| *R76B09* | 33 ± 4 | 53 ± 5 | 20 | 8 | 0.01 | γ(12)4 | β1 | | (α123) | | 3 | BDSC |
| *VT40039* | 47 ± 3 | 67 ± 5 | 20 | 6 | < 0.01 | γ(123)45 | β12 | β'12 | α1 | | 3 | VDRC |
| *NP2397* | 38 ± 3 | 63 ± 7 | 25 | 6 | < 0.01 | γ(3)4(5) | | β'12 | | MB-AIM | X | DGRC-Kyoto |
| *NP7177* | 42 ± 7 | 71 ± 5 | 29 | 6 | < 0.01 | γ(3)4(5) | | β'12 | | MB-AIM | X | DGRC-Kyoto |
| *R24E12* | ND | ND | ND | ND | ND | γ(12)4 | | β'1 | | | 3 | BDSC |
| *NP2119* | ND | ND | ND | ND | ND | γ15 | β(1)2 | β'2 | (α123) | MB-M1/-MVP2 | X | DGRC-Kyoto |
| *NP2755* | ND | ND | ND | ND | ND | γ25 | β12 | β'2 | α2α'12 | MB-MV1 | 2 | DGRC-Kyoto |
| *NP0393* | ND | ND | ND | ND | ND | | | β'2 | | MB-M4 | 2 | DGRC-Kyoto |
| *NP7251* | ND | ND | ND | ND | ND | γ15 | β(1)2 | β'2 | (α123) | MB-M1/-MVP2 | X | DGRC-Kyoto |

Screen data are presented along with Gal4 driver information. In the screen, *UAS-Kir2.1; Gal80$^{ts}$* females were crossed to Gal4 driver males or wild type males ("*no Gal4*"). For X-chromosome-located Gal4 drivers, data were generated from the female progeny; for other Gal4 drivers, the progeny of both sexes were used. Most of the screened Gal4 drivers were expressed in multiple MBEN types and also in other nearby neurons, making it difficult to accurately annotate the MBEN types labeled in each driver. For this reason, the MB lobe compartments covered in the Gal4 expression patterns were examined and used as an approximate estimation of MBEN types. Lobe compartments showing visible but weak expression are marked by brackets; they were not included in the generation of the coverage

pattern in **Fig. 1A** to avoid masking the major compartment information. Abbreviations: s.e.m., standard error of mean; Chr, chromosome; ND, not determined because of lethality or sickness; BDSC, Bloomington *Drosophila* Stock Center, VDRC, Vienna *Drosophila* Resource Center; DGRC-Kyoto, Japan *Drosophila* Genetic Resource Center in Kyoto.

**Table S2. Task-relevant sensorimotor responses**

| Genotype | Treatment | Shock Reactivity (60 V) | Olfactory Acuity | |
|---|---|---|---|---|
| | | | OCT ($1.5\times10^{-3}$) | MCH ($10^{-3}$) |
| *+/Y; UAS-Kir2.1/+; Gal80$^{ts}$/+* | –HS | 67 ± 6 | 66 ± 6 | 70 ± 6 |
| | +HS | 63 ± 5 | 53 ± 11 | 64 ± 8 |
| *NP2397/+; UAS-Kir2.1/+; Gal80$^{ts}$/+* | –HS | 68 ± 5 | 76 ± 8 | 72 ± 9 |
| | +HS | 65 ± 5 | 66 ± 4 | 64 ± 6 |
| *+/Y; UAS-Kir2.1/+; Gal80$^{ts}$/+* | –HS | 69 ± 5 | 56 ± 7 | 73 ± 4 |
| | +HS | 70 ± 3 | 52 ± 9 | 71 ± 7 |
| *NP7177/+; UAS-Kir2.1/+; Gal80$^{ts}$/+* | –HS | 63 ± 3 | 68 ± 8 | 70 ± 6 |
| | +HS | 63 ± 5 | 58 ± 7 | 68 ± 2 |
| *UAS-Kir2.1/+; Gal80$^{ts}$/R76B09* | –HS | 66 ± 2 | 42 ± 4 | 31 ± 4 |
| | +HS | 64 ± 3 | 49 ± 4 | 27 ± 2 |

Sensorimotor responses to electric shock and odors used in the conditioning task were evaluated. For *NP2397* and *NP7177*, data were collected for the –HS and +HS groups of flies of the desired genotype (female) and the driverless siblings (male). These four groups were set up for a comparison and analyzed by one-way ANOVA (For *NP2397*, shock, $p = 0.92$, $n = 7$; OCT, $p = 0.28$, $n = 6$; MCH, $p = 0.81$, $n = 6$; for *NP7177*, shock, $p = 0.50$, $n = 8$; OCT, $p = 0.51$, $n = 6$; MCH, $p = 0.93$, $n = 6$). For *R76B09*, data from the –HS and +HS groups were compared and analyzed by t-test (shock, $p = 0.59$, $n = 8$; OCT, $p = 0.27$, $n = 6$; MCH, $p = 0.47$, $n = 6$). Data are means ± s.e.m.

**Supplementary References**


1. Hayashi S*, et al.* (2002) GETDB, a database compiling expression patterns and molecular locations of a collection of Gal4 enhancer traps. *Genesis* 34(1-2):58-61.

2. Tanaka NK, Tanimoto H, & Ito K (2008) Neuronal assemblies of the Drosophila mushroom body. *J Comp Neurol* 508(5):711-755.

3. Jenett A*, et al.* (2012) A GAL4-Driver Line Resource for Drosophila Neurobiology. *Cell Rep* 2(4):991-1001.

4. Kvon EZ*, et al.* (2014) Genome-scale functional characterization of Drosophila developmental enhancers in vivo. *Nature* 512(7512):91-95.

5. Pfeiffer BD*, et al.* (2008) Tools for neuroanatomy and neurogenetics in Drosophila. *Proc Natl Acad Sci U S A* 105(28):9715-9720.

6. Lai SL & Lee T (2006) Genetic mosaic with dual binary transcriptional systems in Drosophila. *Nat Neurosci* 9(5):703-709.

7. Aso Y*, et al.* (2014) The neuronal architecture of the mushroom body provides a logic for associative learning. *Elife* 3:e04577.